Supplementary Data

LAP-Hsp60 complex modulates the epithelial tight junction barrier

Manalee Samaddar[1,2], Chen Sun[2,3], Nicholas L.F. Gallina[1,2], Nicole Irizarry-Tardi[1,2], Dongqi Liu[1,2], Shivendra Tenguria[1,2,4], Rishi Drolia[1,2,5], Anika Jain[2,3], Daisuke Kihara[2,3], Wen Jiang[2,3], Kee-Hong Kim[2,6], Abigail Cox[2,7], Kurt D. Ristroph[4,8], Gregory T. Knipp[2,9], Nicholas Noinaj[2,3*], Arun K. Bhunia[1,2,7,10*]

[1]Molecular Food Microbiology Laboratory, Department of Food Science, Purdue University, West Lafayette, IN, USA
[2]Purdue Institute of Inflammation, Immunology, and Infectious Disease, Purdue University, West Lafayette, IN, USA
[3]Department of Biological Science, Purdue University, West Lafayette, IN, USA
[4]Department of Agricultural and Biological Engineering, Purdue University, West Lafayette, IN, USA
[5]Department of Biological Science, Old Dominion University, Norfolk, VA, USA
[6]Department of Food Science, Purdue University, West Lafayette, IN, USA
[7]Department of Comparative Pathobiology, Purdue University, West Lafayette, IN, USA
[8]Davidson School of Chemical Engineering (by courtesy), Purdue University, West Lafayette, IN, USA
[9]Department of Industrial and Physical Pharmacy, Purdue University, West Lafayette, IN, USA

*__Corresponding authors__: bhunia@purdue.edu (A.K.B.); nnoinaj@purdue.edu (N.N.)

Supplementary Tables

Supplementary Table 1. Cryo-EM data collection and refinement statistics.

	LAP (dimer)	LAP (tetramer)	Hsp60
Data Collection and Processing			
Magnification	81,000	81,000	81,000
Voltage (kV)	300	300	300
Electron exposure ($e^-/Å^2$)	57.8	54.29	57.8
Defocus range (μm)	1.5 to 2.5	1.5 to 2.5	1.5 to 2.5
Pixel size (Å)	0.527	0.538	0.527
Symmetry imposed	C2	C1	C7
Final particles (no.)	77,918	1,188,837	73,657
Map resolution (Å)	3.20	2.83	3.37
FSC threshold	0.143	0.143	0.143
Map-model CC			
CC_mask	0.78	0.70	0.71
CC_box	0.72	0.56	0.71
CC_peaks	0.68	0.52	0.60
CC_volume	0.75	0.66	0.70
Model Composition			
Non-hydrogen atoms	19,612	32,852	27,461
Protein residues	2,536	4,259	3,682
B factors ($Å^2$)			
Protein	48.59	60.08	119.68
R.M.S. deviations			
Bond lengths (Å)	0.003	0.003	0.003
Bond angles (°)	0.745	0.683	0.705
Validation			
MolProbity Score	2.43	2.29	2.24
Clashscore	12.94	11.49	11.21
Rotamer outliers (%)	3.02	2.32	3.43
Ramachandran Plot			
Favored (%)	93.03	93.24	96.13
Allowed (%)	6.81	6.71	3.87
Outliers (%)	0.16	0.05	0.00
EMDB ID	EMD-49969	EMD-49968	EMD-49967
PDB ID	9O0C	9O0A	9O09
PDB ID (extended)	PDB_00009O0C	PDB_00009O0A	PDB_00009O09
	D_1000294617	D_1000294616	D_1000294623

Supplementary Table 2. PDBePISA analysis of hydrogen bonds between LAP and Hsp60. The three-letter code and atom involved in the bond are shown, and distances are measured in Å.

LAP (Structure 2)	Distance, Å	Hsp60 (Structure 1)
GLN 103 [OE1]	2.29	TYR 201 [OH]
CYS 400 [O]	3.41	HIS 241 [NE2]
GLN 438 [OE1]	3.70	ALA 240 [N]
LYS 391 [NZ]	2.94	ASP 215 [OD1]
THR 104 [OG1]	3.70	SER 258 [O]
LYS 391 [NZ]	2.94	ASP 215 [OD1]
LYS 391 [NZ]	3.81	ASP 215 [OD2]

Supplementary Table 3.

(A) LAP interacting sequence with Hsp60

Designation (amino acid position)	**Location (subdomain)**	**Sequence (total aa)**	**MW**	**pI**	**Net charge at pH 7**	**Water solubility**	**Purity**
Peptide 1 (**P1**) (V97…..E108)	N1	VINEDVQTGVIE (12)	1315.43	0.66	-3	Good	98.15%
Peptide 2 (P2) (K391…..I402)	N2	KAFGIRMKACRI (12)	1393.77	11.39	3.9	Good	98.36%
Peptide 3 (S430…..N444)	C1	SYGKNSVSQNVSATN (15)	1555.6	9.5	1	Poor	Not made
Peptide 3 (P3) (S430…..N444)	C1	*KSYGKNSVSQNVSATN (16)	1711.79	10.4	2	Good	98.34%
Peptide 4 (**P4**) (D628…D639) **Control**	C1	DKENNIKYPLAD (12)	1419.54	4.17	-1	Good	98.18%

*K (Lysine) residue is added to the N-terminal end of Peptide 3 to improve the water solubility score and used in the epithelial permeability experiment (ExPasy).

(B) LAP/AdhE sequence from *Listeria monocytogenes* F4244 AY561824.1) showing the location of each subdomain (N1, N2, C1, C2).

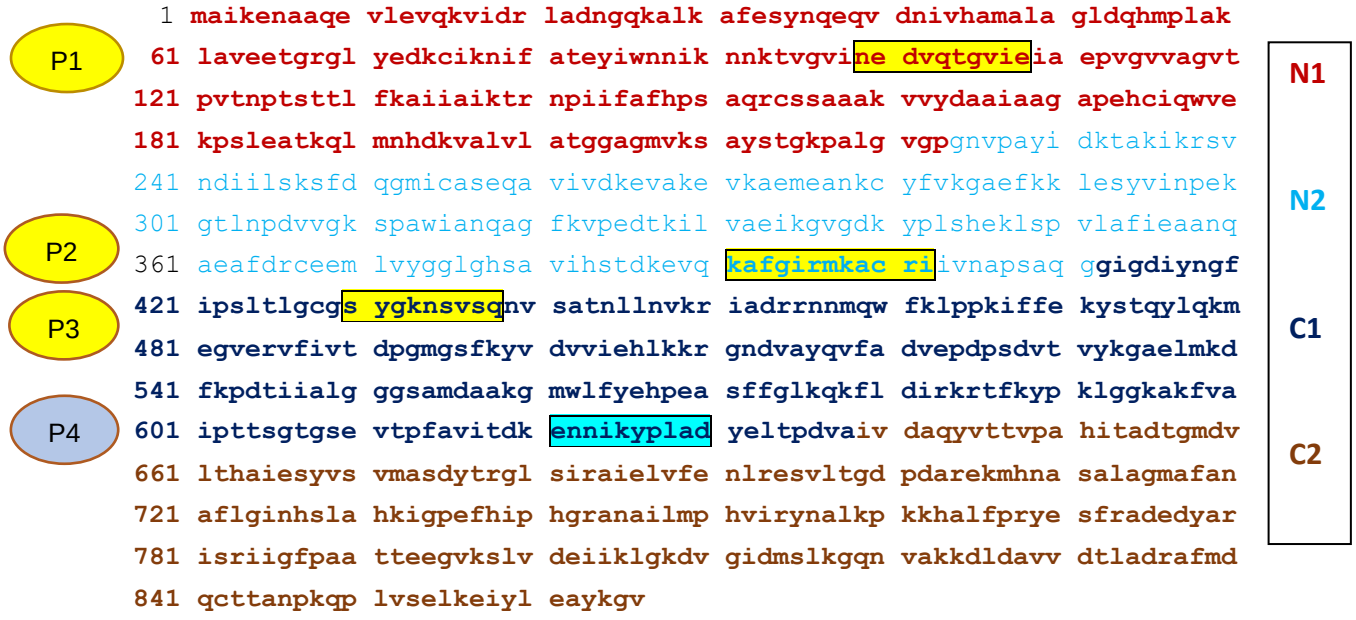

Supplementary Table 4. Biologics used in the study.

Drug Type	Model Drug	Size (Da)	Analysis
Polysaccharide	FD4 (Fluorescein Isothiocyanate conjugated 4 kDa Dextran)	4,000	Spectrophotometer
Polysaccharide	FD40 (Fluorescein Isothiocyanate conjugated 40 kDa Dextran)	40,000	Spectrophotometer
Polysaccharide	FD70 (Fluorescein Isothiocyanate conjugated 70 kDa Dextran)	70,000	Spectrophotometer
Peptide	Vancomycin	1,449	Mass Spec
Peptide	Desmopressin	1,069	Mass Spec

Supplementary Table 5. Summary of LAP-mediated biologics delivery through *in vitro* cell culture and *in vivo* mouse model.

Molecule	Size	Cell line/ Animal Model	Time	Fold Change (with LAP)	Percent Increase (with LAP)
FD4 (Fluorescein Isothiocyanate conjugated 4 kDa Dextran)	4 kDa	Caco-2	20-40 min	3.24	224
		MDCK	40-60 min	3.92	292
		Mouse (C57BL/6)	4 h	18.7 (Serum) 2.05 (Urine)	1649.5 (Serum) 105.6 (Urine)
Vancomycin	~1.4 kDa	Mouse (C57BL/6)	4 h	2.17 (Plasma) 1.54 (Urine)	117.4 (Plasma) 46.2 (Urine)
Desmopressin	~1 kDa	Mouse (C57BL/6)	4 h	UD (Plasma) 3.0 (Urine)	UD (Plasma) 210.6 (Urine)

UD, undetectable

Supplementary Table 6

Reagents	Source	Catalog No.
Antibodies		
Mouse Monoclonal Anti- Claudin 1 (2H10D10)	Thermo Fisher Scientific	Cat # 37-4900
Mouse Monoclonal Anti-Occludin (OC-3F10)	Thermo Fisher Scientific	Cat # 33-1500
Mouse Monoclonal Anti- ZO-1 (ZO1-1A12)	Thermo Fisher Scientific	Cat # 33-9100
Mouse monoclonal anti-E-cadherin	Thermo Fisher Scientific	Cat # 33-4000
Goat anti-rabbit IgG (H+L), F(ab')2 Fragment (Alexa Fluor 488 Conjugate) antibody	Cell Signaling	Cat # 4412
Anti-LAP mAb (mouse)	Our Lab (mAb-H7/ EM-10)	N/A
Anti-N1 (H10) scFv-Fc	Ref [1]	N/A
Anti-N2 (C10) scFv-Fc	Ref [1]	N/A
Anti-C1 (B1) scFv-Fc	Ref [1]	N/A
Anti-C2 (A11) scFv-Fc	Ref [1]	N/A
Bacterial Strains		
L. monocytogenes F4244 (WT)	CDC, Atlanta, GA	N/A
E. coli BL21(DE3) pHIS*I*-LAP	This Study	N/A
E. coli BL21(DE3) pHIS*I*-LAP_N	This Study	N/A
E. coli BL21(DE3) pHIS*I*-LAP_C	This Study	N/A
E. coli BL21(DE3) pHIS*I*-LAP_N1	This Study	N/A
E. coli BL21(DE3) pHIS*I*-LAP_N2	This Study	N/A
E. coli BL21(DE3) pHIS*I*-LAP_C1	This Study	N/A
E. coli BL21(DE3) pHIS*I*-LAP_C2	This Study	N/A
E. coli BL21(DE3) pHIS*I*-Hsp60_FL	This Study	N/A
E. coli BL21(DE3) pHIS*I*-Hsp60_TR	This Study	N/A
Plasmid/Vector		
pHIS2	Addgene	
Chemicals, Peptide/protein		
Uranyl acetate	SPI	Cat # 6159-44-0
LB (Luria Bertani) broth	RPI	Cat # L24060
2XYT	RPI	Cat # X15600
BHI (brain Heart Infusion)	RPI	Cat # B11000
Phusion® High-Fidelity DNA Polymerase	NEB	Cat# M0530
NcoI	NEB	Cat# R0193
XhoI	NEB	Cat# R0146
PMSF Protease Inhibitor	Thermo Fisher	Cat# 36978
IPTG	RPI	Cat# 367-93-1
Pierce™ BCA Protein Assay Kit	Thermo Fisher	Cat# 23225
Pierce™ Chromogenic Endotoxin Quant Kit	Thermo Fisher	Cat#A39552S
Hsp60 (Human Recombinant)	Cayman	Cat# 22738
Vancomycin hydrochloride	Fisher Scientific	Cat # AC296990010
Desmopressin	RnD System	Cat # 3396/1
FITC-labeled 4 kDa dextran	Sigma-Aldrich	Cat # 46944

FITC-labeled 40 kDa dextran	Sigma-Aldrich	Cat # 60842-46-8
FITC-labeled 70 kDa dextran	Sigma-Aldrich	Cat # 60842-46-8
DMEM	GE Healthcare	Cat # D6429
RPMI	Sigma	Cat # R8758
FBS	R&D System	Cat # S11150
DAPI	Cell Signaling	Cat # 4083
Phalloidin (Alexa Fluor 555 Conjugate)	Thermo Fisher Scientific	Cat # A34055
Mouse CRP ELISA kit	Sigma-Aldrich	Cat # RAB1121
Mouse IL-6 ELISA Kit	Sigma-Aldrich	Cat # RAB0308
Mouse TNF-α ELISA Kit	Sigma-Aldrich	Cat # RAB0477
Mouse Lipocalin Assay Kit	R&D System	Cat # DY1857-05
Pepsin	Sigma-Aldrich	Cat # P7125
Pancreatin	Sigma-Aldrich	Cat # P3292
KCl	Fisher Scientific	Cat # P217-500
KH_2PO_4	Thermo Fisher Scientific	Cat # 011594-36
$NaHCO_3$	Thermo Fisher Scientific	Cat # 014707-A3
NaCl	Fisher Scientific	Cat # S271-500
$MgCl_2 \cdot 6H_2O$	Thermo Fisher Scientific	Cat # 036226-36
$(NH_4)_2CO_3$	Fisher Scientific	Cat # S25166
HCL	Fisher Scientific	Cat # SA48-1
$CaCl_2$	Fisher Scientific	Cat # AC349615000
Experimental Models: Cell Lines		
Cell line: Caco-2	ATCC	Cat # HTB37
Cell line: MDCK	ATCC	Cat # CCL-34
Experimental Models: Organisms/Strains		
Mouse: C57BL/6	Charles River	Strain # 243
MLCK knockout	Ref [2,3]	N/A
Oligonucleotides		
LAP_N1_F AAACCATGGCAATTAAAGAAAATGCGGCCC	This Study	N/A
LAP_N1_R TTTCTCGAGTTATGGTCCAACACCTAGTGCAGG	This Study	N/A
LAP_N2_F AAACCATGGGTAACGTACCAGCTTACATTG	This Study	N/A
LAP_N2_R TTTCTCGAGTTAGCCTTGTGCGCTTGGTGC	This Study	N/A
LAP_C1_F AAACCATGGGTATCGGTGACATTTATAACGGC	This Study	N/A
LAP_C1_R	This Study	N/A

TTTCTCGAGTTAAACAGTAGTTACATATTGTGC		
LAP_C2_F AAACCATGGCACACATTACTGCTGACACTGG	This Study	N/A
LAP_C2_R TTTCTCGAGTTAAACACCTTTGTAAGCTTCTAGG	This Study	N/A
Hsp60_FL_F AAACCATGGGACTTCGGTTACCCACAGTC	This Study	N/A
Hsp60_FL_R AAACTCGAGTTA GAACATGCCACCTCCC	This Study	N/A
Hsp60_TR_F AAACCATGGGA GCCGATGCTGTGGCCGTTAC	This Study	N/A
Hsp60_TR_R AAACTCGAGTTA AGGGTCCTTCTCTTCTTTAGG	This Study	N/A
Synthetic Peptides Derived from LAP		
Peptide 1 (N99…E108): VINEDVQTGVIE	NovoPep	http://www.novopep.com/
Peptide 2 (K391…I402): KAFGIRMKACRI	NovoPep	http://www.novopep.com/
Peptide 3 (S430…N444): **K**SYGKNSVSQNVSATN	NovoPep	http://www.novopep.com/
Peptide 4 (E630…D639): DKENNIKYPLAD	NovoPep	http://www.novopep.com/
Software and Algorithms		
BioRender	BioRender	https://www.biorender.com
SnapGene	GSL Biotech	https://www.snapgene.com
UCSF ChimeraX	UCSF v1.3	https://www.cgl.ucsf.edu/chimera/
Relion Cryo EM	RELION v 3.1	https://www.linuxvixion.com/software/relion/
CryoSPARC	CryoSPARC v4.4.0	https://cryosparc.com
Alpha fold	Alpha fold 2	https://github.com/google-deepmind/alphafold
GraphPad Prism 8	GraphPad Software	https://www.graphpad.com/scientific-software/prism/
Microsoft Excel	Microsoft	https://products.office.com/en-us/excel
MaxQuant	MaxQuant	https://www.maxquant.org

Nikon Elements	Nikon	https://www.nikoninstruments.com/Products/Software/NIS-Elements-Basic-Research
FIJI	NIH	https://imagej.nih.gov/ij/

Supplementary Figures

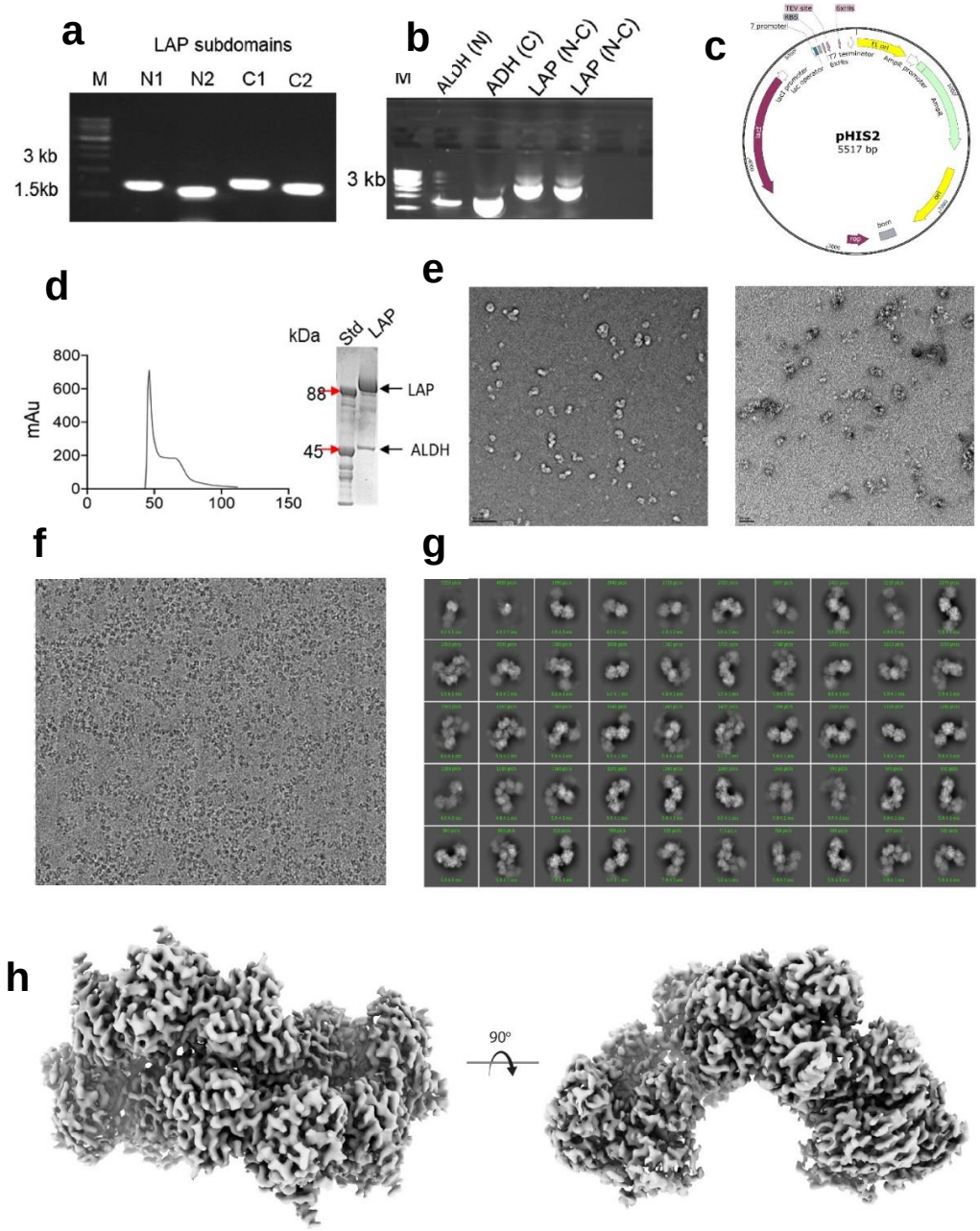

Supplementary Fig. 1. Cloning and structure determination of LAP.

a-b. Agarose gel images of LAP clones and its four subdomains (N1, N2, C1, C2) and N and C domains.

c. Vector Map (pHIS2 parallel).

d. LAP eluted across a broad molecular weight range in Superdex 200 size exclusion chromatography. SDS-PAGE images of LAP showing protein purity. Full-length LAP (94 kDa) and ALDH (47 kDa) (b). Note ALDH was confirmed by N-terminal sequencing by the Edman degradation method.

e. Representative micrographs of negative-stain EM analysis of LAP.

f. Micrograph from the cryo-EM data collection showing homogenous well-separated particles. **g**. Select 2D classes from the 2D classification showing excellent detailed projections of the LAP structure at various orientations.

h. Cryo-EM maps of LAP in different orientations.

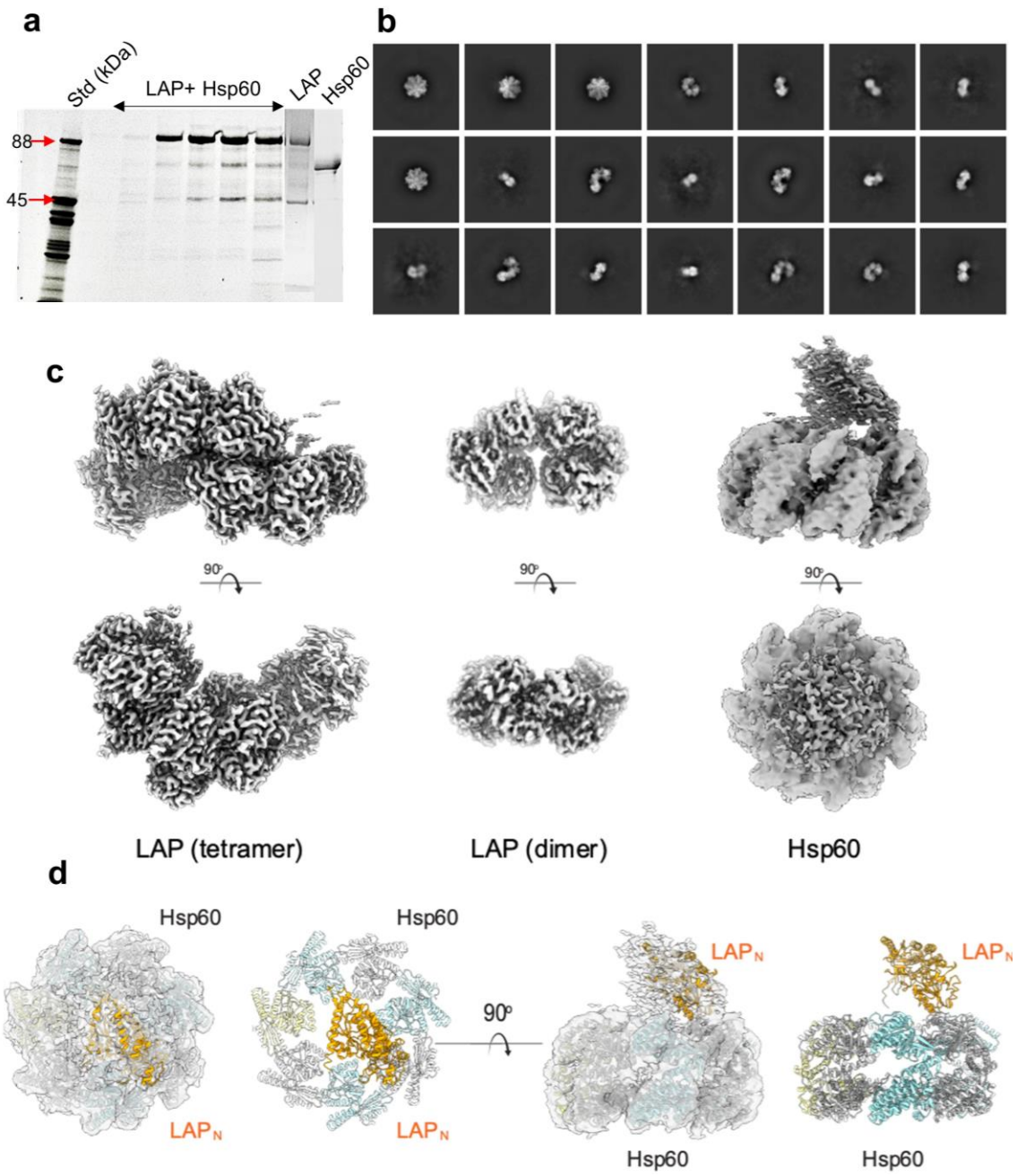

Supplementary Fig. 2. Structure determination of LAP-Hsp60 complex using cryo-EM.
a. SDS-PAGE analysis of the peak fractions of the LAP-Hsp60 complex following SEC.
b. Top 2D classes from the 2D classification showing at least three different structures consistent with Hsp60, LAP tetramer, and LAP dimer.
c. The cryo-EM maps of the LAP tetramer, LAP dimer, and Hsp60 at orthogonal views. The contour of Hsp60 is reduced in order to show the extra density, which may represent the N-terminal domain of LAP.
d. Model of the LAP-Hsp60 complex at orthogonal angles showing the interaction of the N-terminal domain of LAP interaction along the top edge of the interface between Hsp60 multimers.

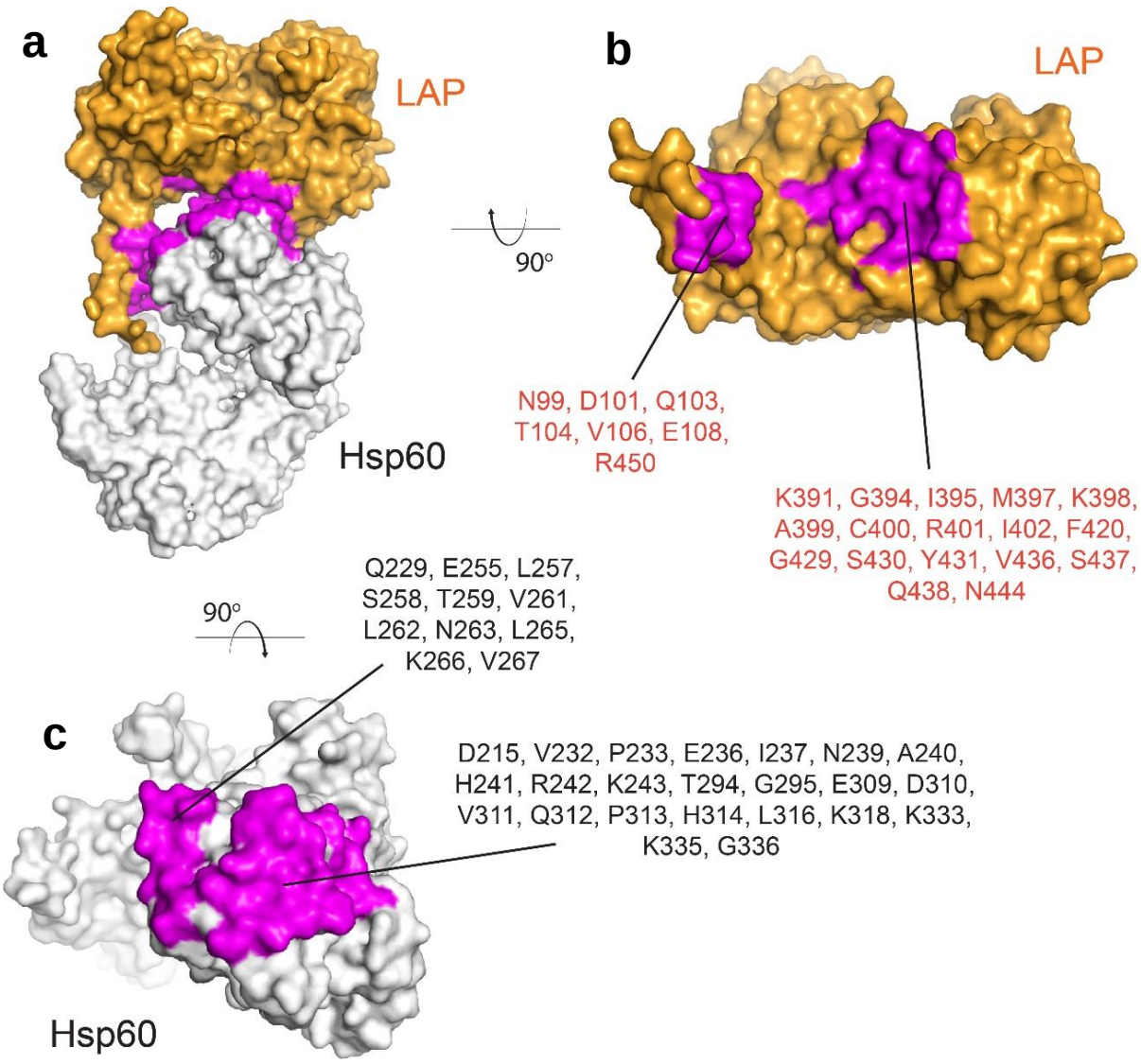

Supplementary Figure 3. The interaction interface of LAP and Hsp60.
a. Based on the ePISA analysis, the interacting residues mediating the interaction of LAP (orange) with Hsp60 (gray) were mapped to the surface of each of the structural models.
b. The structure of LAP (orange) with the residues interacting with Hsp60 in magenta.
c. The structure of Hsp60 (gray) with the residues interacting with LAP colored in magenta.

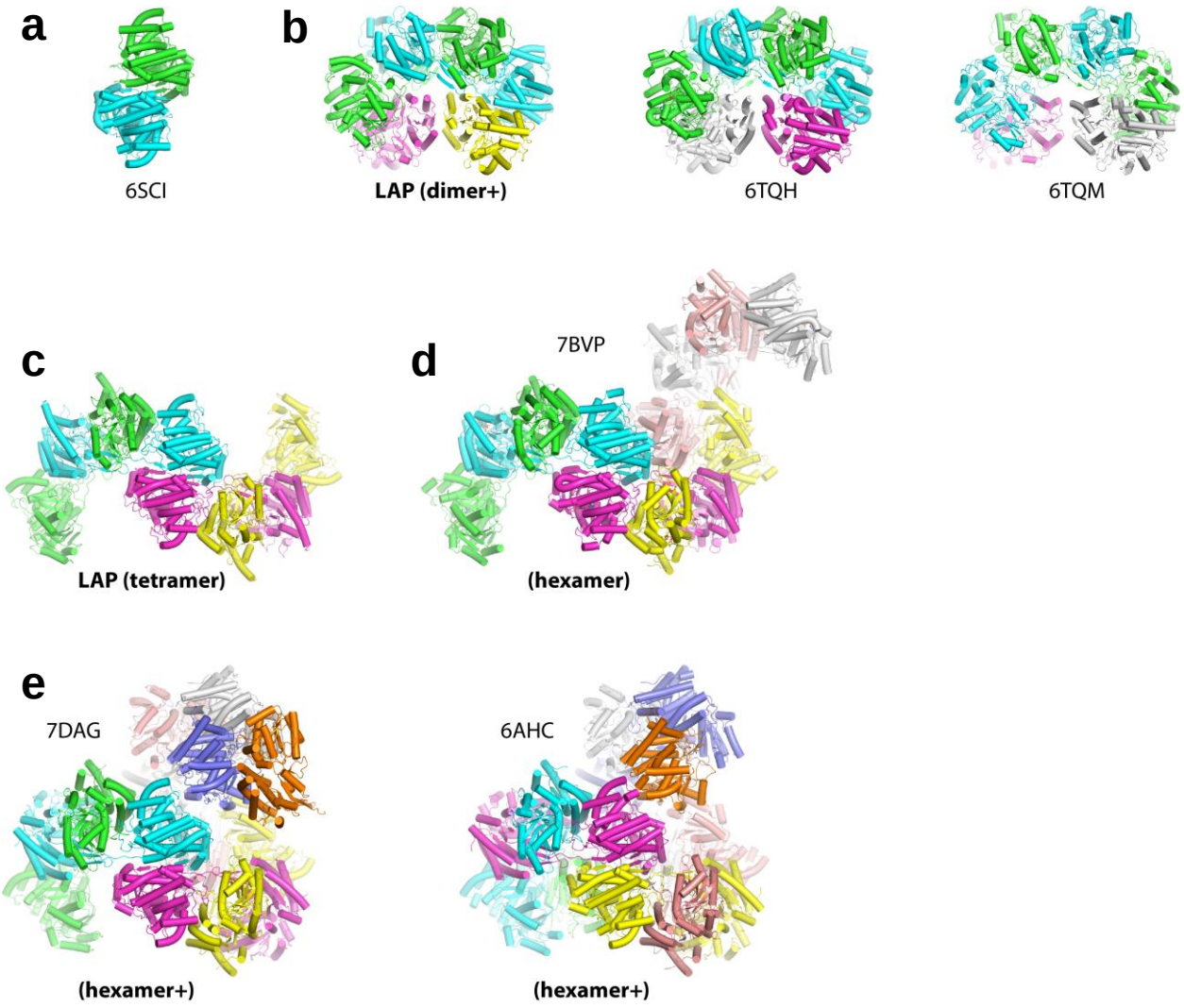

Supplementary Fig. 4. Structural comparisons of LAP to the *E. coli* AdhE structures. **a-e.** LAP has an overall comformation shared with recently solved structures of acetaldehyde alcohol dehydrogenase (AdhE). Similar to LAP, which was found in multiple oligomeric states, AdhE has been observed as a homodimer with just the C-terminal alcohol dehydrogenase domain (**a**), a dimer of the full-length construct (**b**), and hexamers and larger assemblies (**d, e**). LAP has also been observed as a tetramer (**c**). The dimeric interface observed in the crystal structure of the C-terminal domain (**a**) is shared in the larger oligomers, supporting that this is the interface that mediates the formation of the larger oligomer (**b, c, d, e**). PDB IDs are indicated for the respective structures.

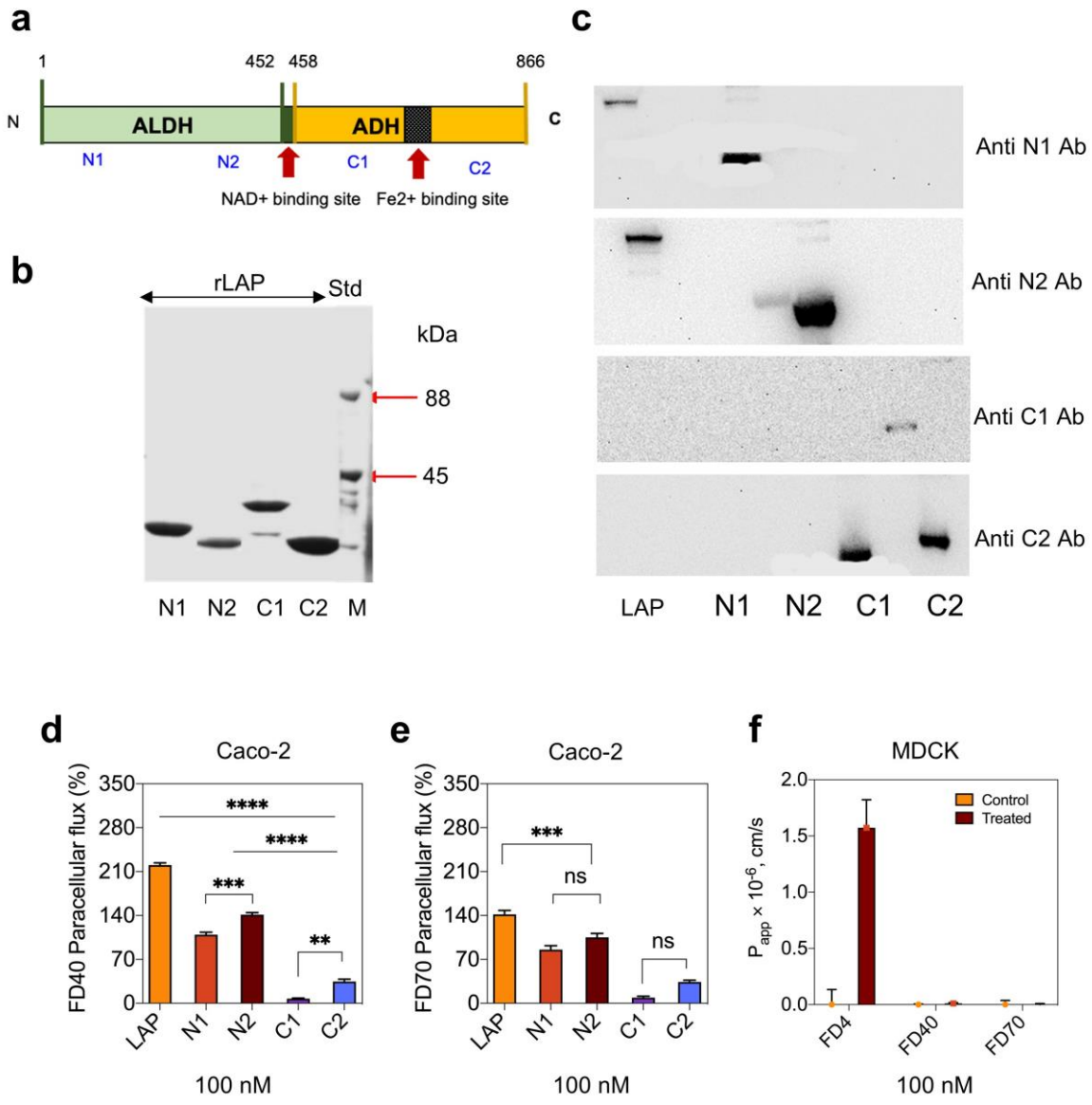

Supplementary Fig. 5. LAP and subdomains (N1 and N2) increase the epithelial permeability to molecules of different sizes.

a. Schematics of LAP (866 aa) showing the location of each subdomain.

b. SDS-PAGE analysis showing purity of each subdomain protein.

c. Western blot showing reactivity of each subdomain protein immunoprobed with single chain antibody[1].

d-e. LAP and subdomains (N1, N2, C1 and C2)-mediated translocation of FD40 (D) and FD70 (E) permeability through Caco-2 cell monolayers in transwell in 1 h.

f. Comparison of apparent permeability coefficient (P_{app}) of LAP-mediated translocation of FD4, FD40 and FD70 in MDCK cell line.

All error bars represent SEM (n = 3). ****p < 0.0001; ***p < 0.001; **p < 0.01; ns, no significance.

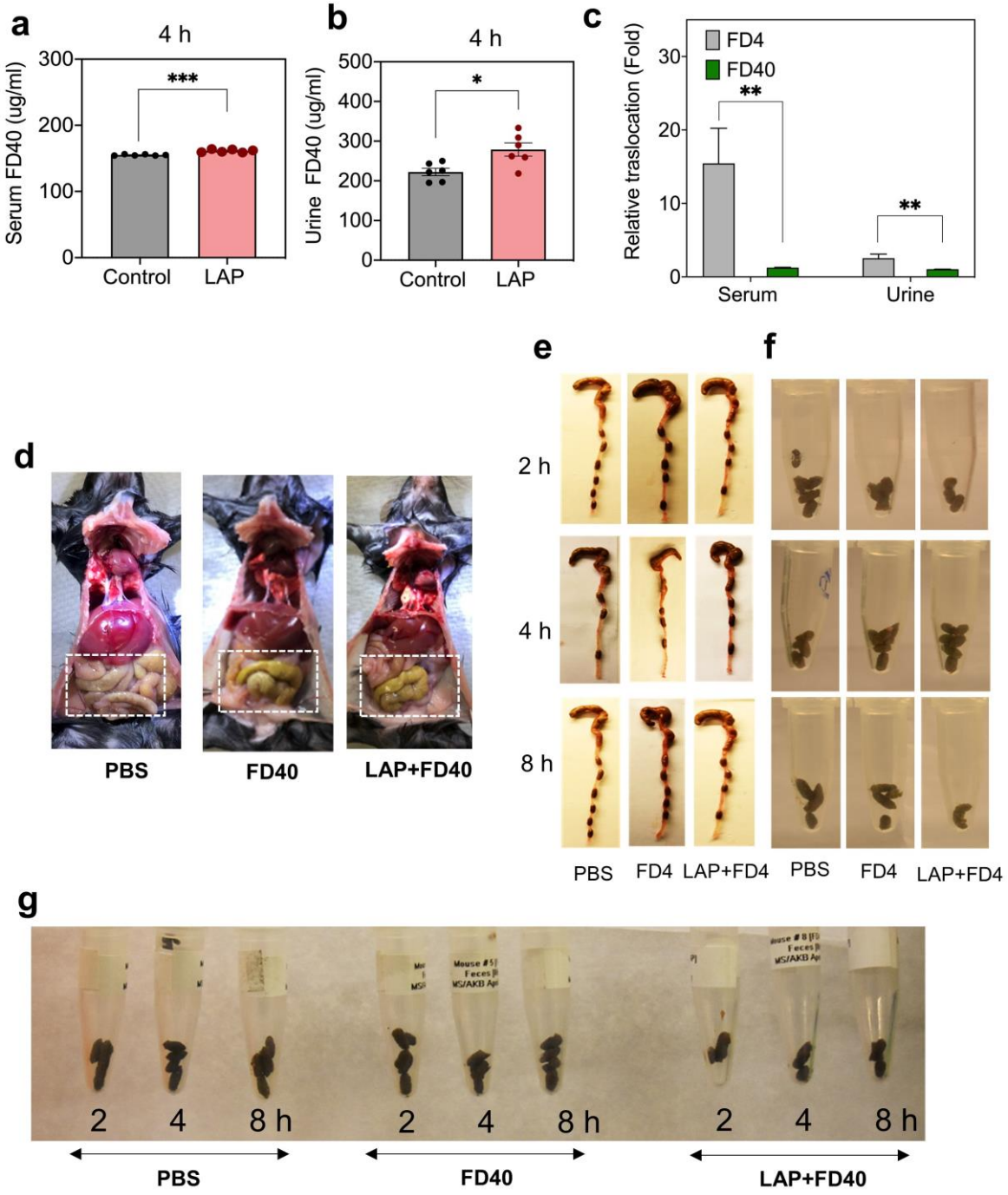

Supplementary Fig. 6. LAP follows the leak pathway during the oral delivery of biologics.
a-b. FITC-40-kDa dextran (FD4) permeability in serum and urine of mice at 4 h.
c. Comparison of relative permeabilty between FD4 and FD40 in mice (4 h).
d. Gross appearance of the intestine and internal organs of mice 4 h post gavage.
e-g. Gross appearance of cecum and colon (E), and feces (F,G) of mice 2, 4 and 8-h-post gavage.

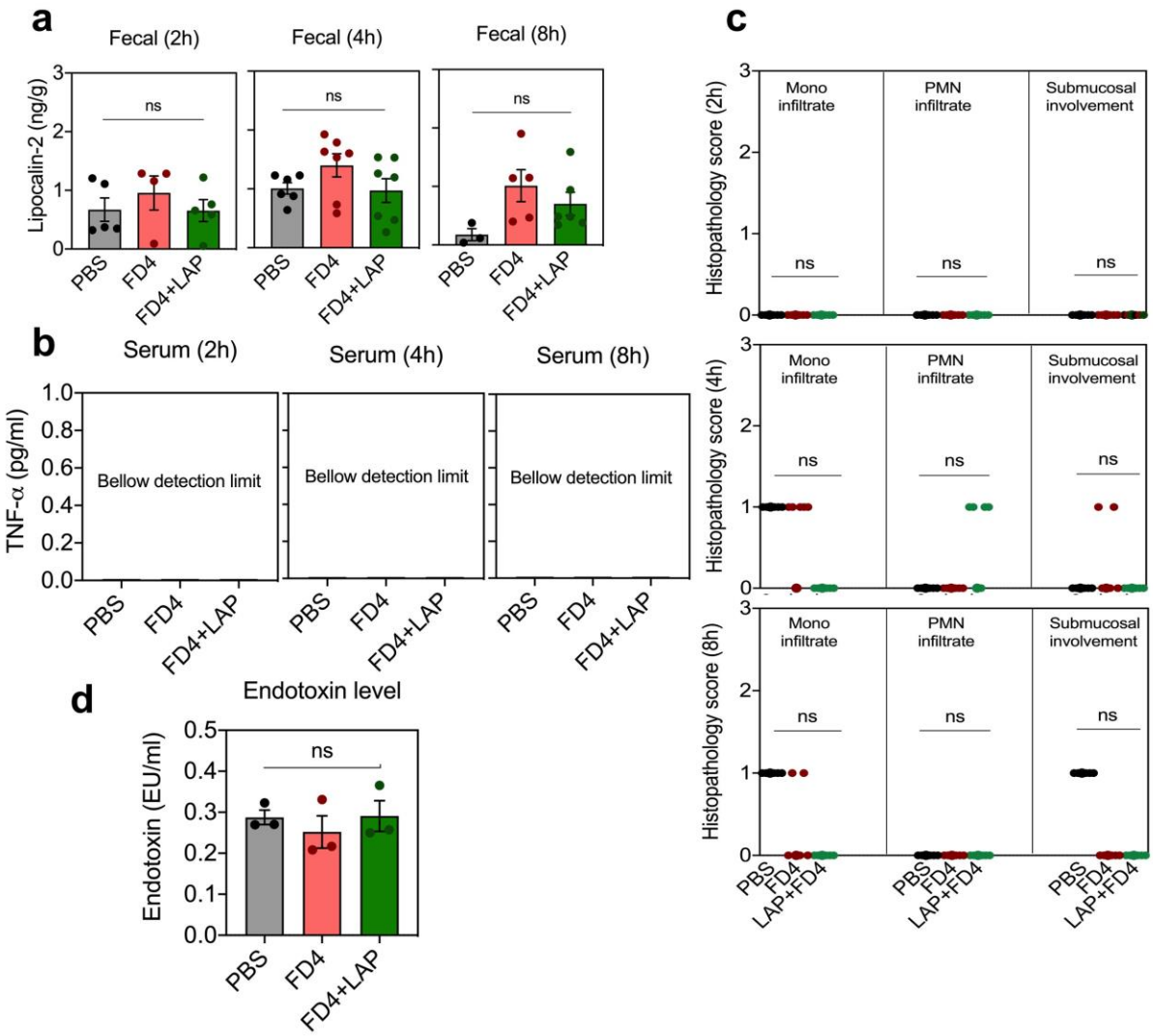

Supplementary Fig. 7. Analysis of inflammation markers in fecal and serum samples of mice upon LAP treatment.

a-b. ELISA analysis of fecal lipocalin-2 (a) and serum TNF-α (b) in mice at 2, 4, and 8-h post gavage.
c. Histopathology score of ileal sections after 2, 4 and 8 h of LAP treatment. Score details for mononuclear cells, polymorphonuclear infiltrate and submucosal involvement are as follows: 3 = markedly increased, 2 = moderately increased, 1 = slightly increased, 0 = normal.
d. Endotoxin analysis of mice serum sample after 4 h of LAP treatment.
All error bars represent SEM (n = 3-4). ns, no significance.

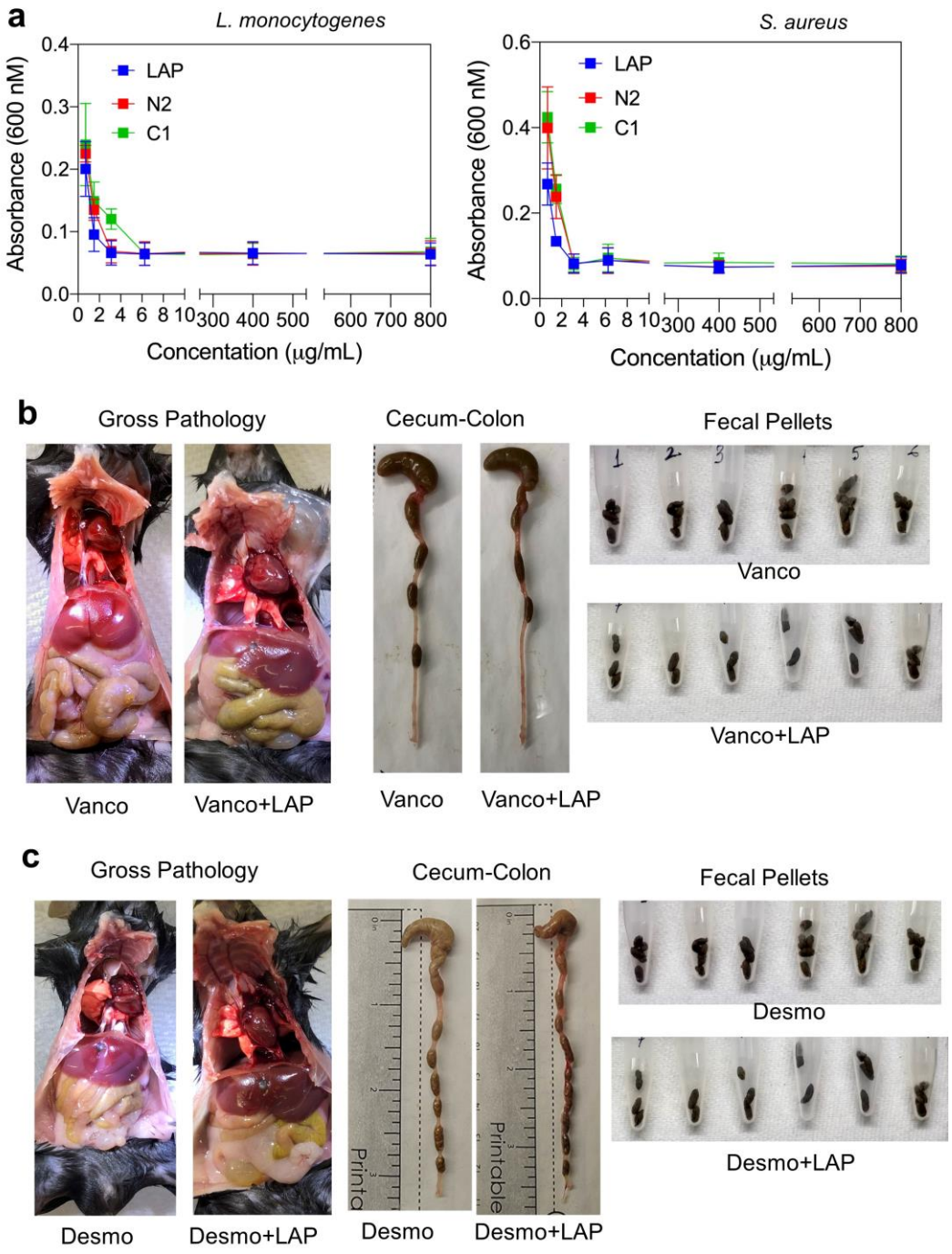

Supplementary Fig. 8. Oral delivery of peptide drugs using LAP as an excipient in mice.
a. Estimating minimum inhibitory concentration (MIC) of vancomycin and LAP (N2 and C1) mixture against *Listeria monocytogenes* and *Staphylococcus aureus*.
b-c. Gross appearance of the gastrointestinal tract and internal organs, cecum-colon and fecal pellets in mice orally gavaged with vancomycin (b) and desmopressin (c). (n=6 animals per treatment).

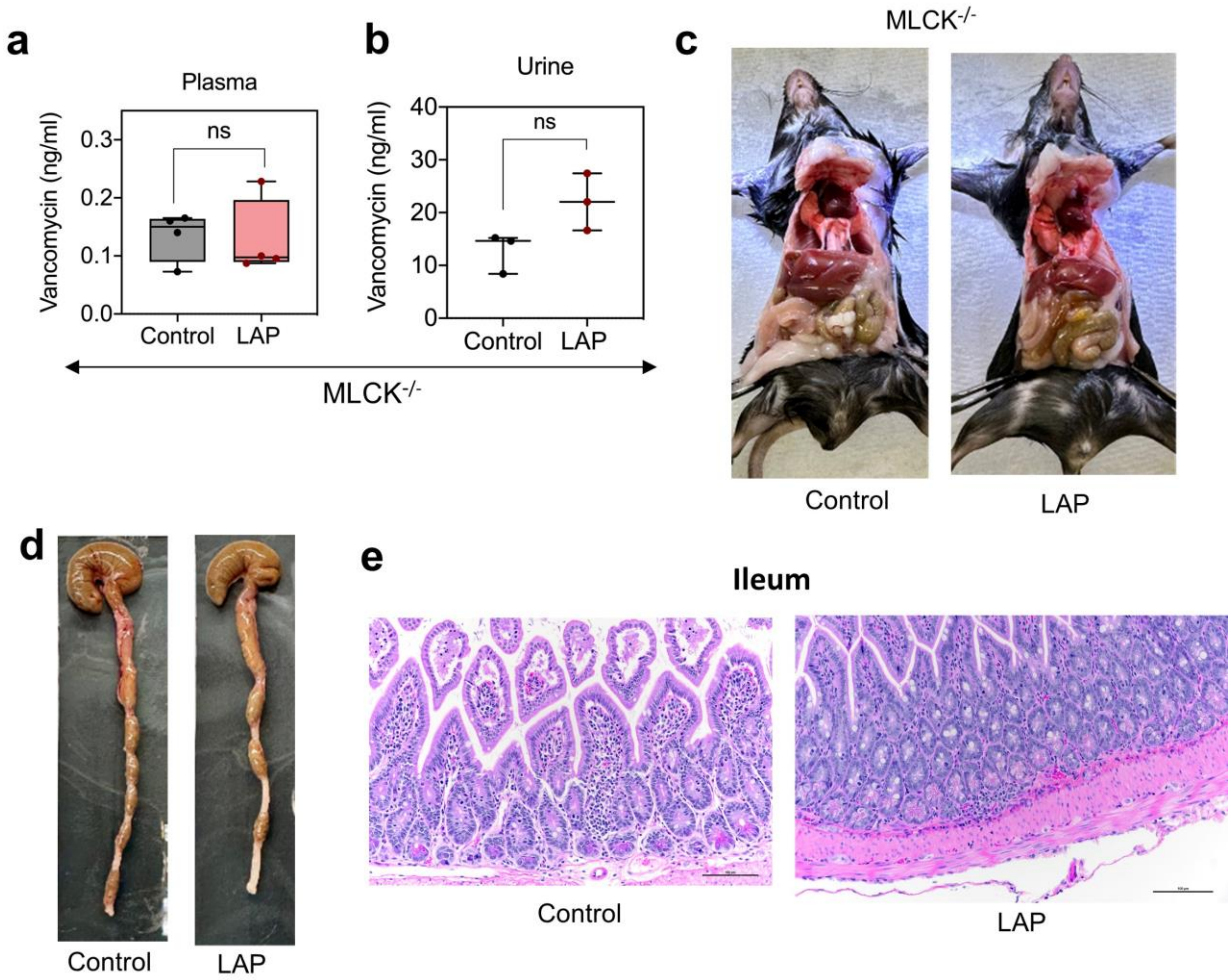

Supplementary Fig. 9. LAP did not increase epithelial permeability in myosin chain kinase (MLCK) knock-out mice.

a-b. Levels of vancomycin and desmopressin concentration in mice (MLCK$^{-/-}$) plasma (a) and urine (b) at 4 h after oral gavage of vancomycin with LAP. Control animals received only vancomycin. (N=4).

c-d. Gross appearance of the gastrointestinal tract and internal organs (c), and cecum-colon (d) in mice orally gavaged with vancomycin of the 4-h-post gavage.

e. Hematoxylin and eosin (H&E)-stained histopathological images of mouse ileal tissue sections.

All error bars represent SEM. ns, no significance.

Supplementary movies

Supplementary Movie 1. LAP monomer, dimer and tetramer.

Supplementary Movie 2. LAP (N1 + N2) interaction with Hsp60.

Supplementary Movie 3. A model for the InlB-LAP-Hsp60 intercellular adhesion complex.

Supplementary Movie 4. Occludin expression in mice ileal tissue after 4 h of oral gavage of LAP showed controlled TJ protein disruption.

References

1. Liu, D.*, et al.* Cell-surface anchoring of *Listeria* adhesion protein on *L. monocytogenes* is fastened by internalin B for pathogenesis. *Cell Reports* **42**, 112515 (2023).
2. Clayburgh, D.R.*, et al.* Epithelial myosin light chain kinase–dependent barrier dysfunction mediates T cell activation–induced diarrhea in vivo. *J. Clin. Invest.* **115**, 2702-2715 (2005).
3. Drolia, R., Tenguria, S., Durkes, A.C., Turner, J.R. & Bhunia, A.K. *Listeria* adhesion protein induces intestinal epithelial barrier dysfunction for bacterial translocation. *Cell Host & Microbe* **23**, 470-484 (2018).